this is a relatively simple matter. Gathering of such data will assist with development of criteria for design.

CONCLUSIONS

Details of measured results of stresses and deflections associated with extremely heavy live loading of large-span corrugated-metal arches have been presented. In addition, the permanent effects of these loads on the deflection response have been demonstrated and discussed. Further research in this area will be necessary to enable proper consideration of heavy live loading in the design phase.

REFERENCE

1. J.N. Kay, D.L. Avalle, R.C.L. Flint, and C.F.R. Fitzhardinge. Instrumentation of a Corrugated Steel-Soil Arch Overpass at Leigh Creek, South Australia. Proc., 10th Conference of Australian Road Research Board, Vol. 10, No. 3, 1980, pp. 57-70.

Publication of this paper sponsored by Committee on Subsurface Soil-Structure Interaction.

Response of Corrugated-Metal Arches to Soil Loads

R.C.L. FLINT AND J.N. KAY

To enable prediction of the response of systems with corrugated-metal arches and compacted soil bridges to soil loading above crown level, graphs were developed from a large number of finite-element analyses. The graphs are based on analysis of a flexible arch in the form of a half ellipse supported on either side by typical footings. They facilitate prediction of response parameters as the fill is placed and compacted in layers above the crown level. The material surrounding the arch is considered homogenous in terms of elastic modulus and Poisson's ratio. Although the graphs are based on linear analysis, important nonlinear effects may be taken into account by application of the graphs in a stepwise manner. Comparison of predicted response with that from a specific finite-element analysis of a field structure suggests that the errors introduced by idealizations associated with the graphical approach may be insignificant for many projects. In addition, comparisons of predictions with field measurements show encouraging results.

Large-span corrugated-metal arch structures are becoming more common as an alternative to conventional bridges for rail or highway overpasses spanning minor roads or small waterways. Current installations use spans up to about 15 m (50 ft), and several with spans around 12 m (40 ft) have been constructed in Australia. The corrugated plate used is typically 3-7 mm (1/8 to 5/16 in) thick, depending on the size of the arch, with 150x50-mm (6x2-in) corrugations.

The response of these structures to loading is governed by an interaction between a flexible membrane (corrugated metal) and a relatively compressible surrounding medium (compacted soil fill). Analysis of such systems is difficult due to the complex interaction mechanisms involved. No closed-form solution can adequately approximate the true behavior. Most manufacturers use design methods based on formulas that assume a grossly simplified system but at the same time have the backing of considerable experience. Others have developed empirical methods based on small-scale model studies. Some discussion of these methods has been provided by Selig and others (1).

The finite-element method has now been developed to the extent where models for soil-structure interaction problems may be formulated to provide an adequate means for analysis of these structures under working loads. A number of large-span corrugated-metal arch systems have been individually analyzed by this method (2-4), and the results appear to show acceptable correlation with field measurements. However, the cost associated with such analysis is high, due largely to the time involved in formulating and checking the input data for finite-element programs as well as the actual computing costs. Access to a large computer is also required and is not always available to the design engineer.

This paper presents a method whereby the designer may reap the benefits of the finite-element method without the need to resort to the costly detailed analysis of individual structures. Design graphs based on numerous finite-element analyses are presented that may be used to predict the essential response parameters required for design of the wide range of structural configurations likely to be encountered in practice.

To demonstrate the validity and versatility of the graphs, response predictions based on the graphs are compared both with measured results from a field structure and with results obtained from a specific finite-element analysis of the field structure by using mesh data to more accurately fit the specific field conditions. Subject to the uncertainty associated with determination of the appropriate soil modulus, the results are promising.

CONFIGURATION AND CONSTRUCTION CONSIDERATIONS

Although many full-ellipse structures have been completed, the trend in Australia in recent years has been toward construction of half-ellipse and low-profile arch structures. These appear to be more practical and more economical, particularly for overpass applications. Consequently, the half-ellipse profile has been selected as the basic geometry around which the graphs are developed.

The arch is constructed from curved corrugated-plate sections approximately 2x1 m (6x3 ft), which are bolted together on site. Profiles close to elliptical are formed from circles of two different radii for the top and side arch sections. The junction of the two circles occurs at the point where the two radii have a common angle of 50 degrees to the horizontal.

It is convenient to subdivide the construction operation into two stages--stage 1, where the arch is erected and the fill is placed and compacted to crown level, and stage 2, where the fill above the crown is placed and compacted to finished level. The response of the structure to loading during stage 1 is largely dependent on the construction techniques employed. Up to this time, engineering

Figure 1. Diagram of notation.

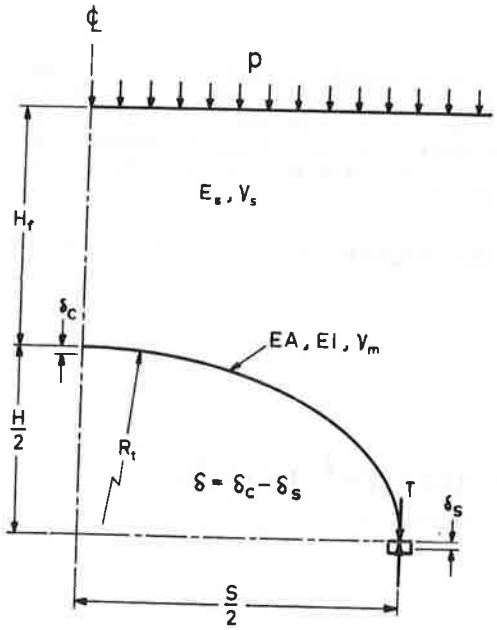

computation has provided little assistance, and an on-site trial-and-error approach in accordance with specified tolerances appears to be the best approach.

For the second stage (placement and compaction of fill above the crown level), the response of the system is considerably less dependent on construction effects and can be treated in terms of fundamental engineering mechanics. Fortunately, provided the specifications on system geometry are achieved in stage 1, the loading and the response during the second stage and after govern the in-service safety of the structure.

Widespread practice in corrugated-metal arch construction is to incorporate thrust beams. These are concrete beams running longitudinally along the shoulder of the arch on either side near the change in plate radius. The beams are cast in situ directly on the corrugated metal and are fixed to the arch by shear connectors. It is widely accepted that thrust beams serve to provide a nearly vertical wall against which the side fills may be compacted to a high standard without severely distorting the arch. They constitute an easily placed comparatively rigid material in this critical region where it is difficult to obtain satisfactory soil compaction.

Based on these considerations, the procedure presented in this paper covers prediction of response due to loading imposed during stage-2 construction for a semielliptical structure that incorporates thrust beams.

FAILURE CRITERIA

Failure of large-span corrugated-metal arch structures has been observed to occur by either of two modes. The first involves a snap-through type buckling failure of the top section of the corrugated-metal arch and is obviously of a catastrophic nature. The second involves seam failure of the corrugated-metal arch wall and is most likely to occur at the springline where the tangential thrust is greatest. In some cases, seam failure may be repairable, but in others it may be associated with catastrophic collapse.

For a design to be satisfactory, the system must exhibit an acceptable factor of safety against both modes of failure. The proposed procedure entails prediction of structural response under working load. This may be compared with acceptable limits derived from consideration of the failure mechanisms. The seam-failure mode is a relatively simple matter associated with the tangential thrust in the arch wall. However, the snap-through buckling mode is much more complex. For small circular pipes, Spangler (5) considered excessive deflection to be the logical criterion for such failure and suggested a maximum safe change in diameter of 5 percent. This is based on laboratory tests that indicated a collapse condition when deflection reached about 20 percent of the diameter. No comprehensive study of this collapse mechanism has yet been made for large-span corrugated-metal arch systems, and no limits for safe deflections based on rational analysis of the problem are available (6). However, control of deflection would appear to be the most promising approach.

METHODS OF ANALYSIS

The method presented enables calculation of the structural response associated with a uniformly distributed load applied on a level surface at any height above crown level. Nonlinear effects may be taken into account by analyzing any given problem in a stepwise fashion that simulates fill placement in the field. For analysis, the fill to be placed above crown level is divided into a number of layers. The load equal to the overburden pressure imposed by the layer is applied to the system with the upper boundary level at the layer mid-height. The structural response resulting from this load is then determined from the graphs.

By summing the contributions from successive layers, the total structural response as fill is placed above crown level is determined.

The parameters used to describe the behavior of the system are illustrated in Figure 1. The top radius (R_t) associated with the circle approximations to the ellipse is uniquely related to the major and minor diameters (S and H, respectively) by the following:

$$R_t = 0.937S - 0.437H.$$

The two key response parameters--the relative crown deflection (δ) and the springline thrust (T)--are some function of the input parameters:

$$\delta = f_\delta(E_s, \nu_s, EA, EI, \nu_m, H, S, R_t, H_f, p) \quad (1)$$

$$T = f_t(E_s, \nu_s, EA, EI, \nu_m, H, S, R_t, H_f, p) \quad (2)$$

where

A = cross-sectional area of arch-wall material per unit length,
E = elastic modulus of material in arch wall,
E_s = elastic modulus of compacted fill,
H_f = height of fill above crown level,
I = moment of inertia of arch-wall material per unit length,
p = uniform soil load per unit area,
ν_s = Poisson's ratio of compacted fill, and
ν_m = Poisson's ratio of arch-wall material.

It has been demonstrated elsewhere (6) that these equations may be written efficiently in dimensionless form as follows:

$$\delta E_s/pR_t = f'_\delta[(H_f/R_t), (E_sR_t/EA), (E_sR_t^3/EI), (S/H), \nu_s, \nu_m] \quad (3)$$

Figure 2. Typical finite-element mesh used for development of graphs.

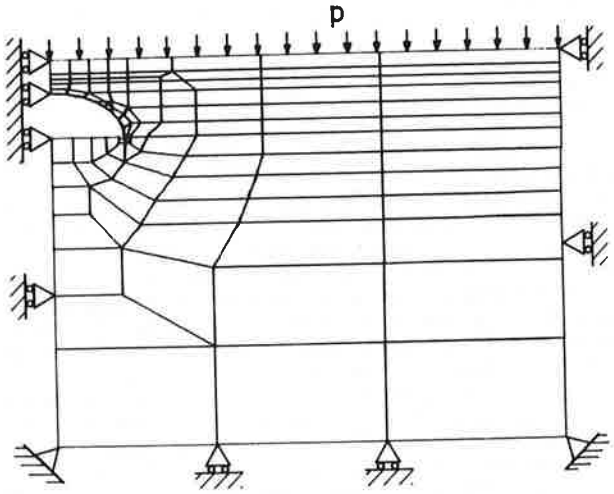

Figure 3. Range of standard arch dimensions available from major supplier.

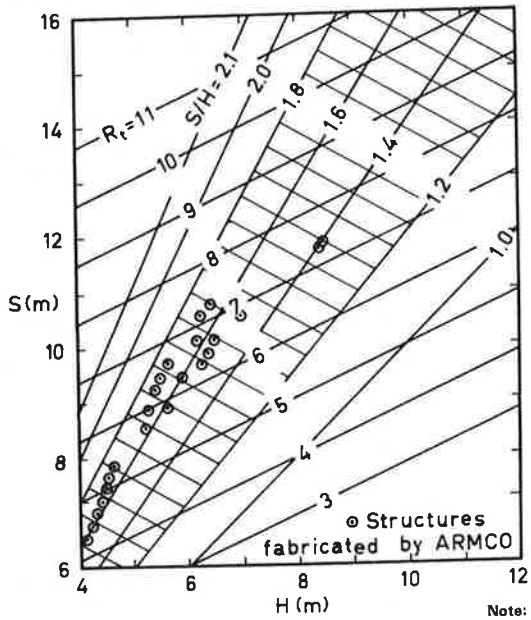

$$T/pR_t = f_f[(H_f/R_t), (E_sR_t/EA), (E_sR_t^3/EI), (S/H), \nu_s, \nu_m] \quad (4)$$

The realistic range for values of each of these dimensionless parameters has been determined, and finite-element analyses of specific structures exhibiting values over the entire range of possible combinations have been performed. The results of these analyses have been used to prepare curves that then provide a graphical solution to Equations 3 and 4.

Once the dimensionless response parameters $\delta E_s/pR_t$ and T/pR_t have been determined from the charts, substitution of the original values of E_s, p, and R_t yields the values of the actual response parameters δ and T.

FINITE-ELEMENT ANALYSIS

The two-dimensional finite-element program Elaspipe (2) was used for the parameter studies. The program employs rectangular, quadrilateral, and triangular elements to represent the soil. The formulations

Figure 4. Range of flexibility parameter combinations corresponding to current practice.

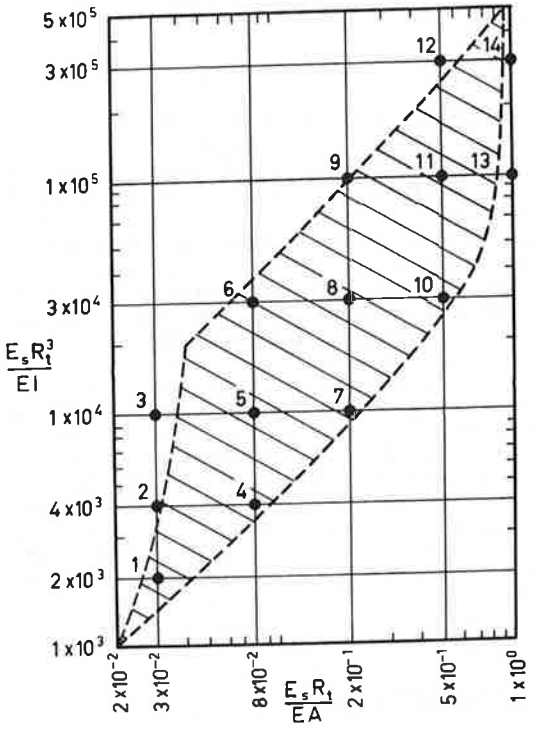

for these types of elements are, respectively, the Q6, Q4, and CST formulations. The pipe is represented by a series of elliptical, cubic-displacement bending and stretching elements with independently specified flexural and axial stiffnesses. All analyses assume linear-elastic, plane-strain conditions.

Figure 2 shows a typical element mesh. The problem is symmetrical about the vertical centerline, and the boundaries as shown are clear of the influence of the arch. Top layers of elements are added or removed as appropriate for different cover heights. Note that the only load applied is the uniformly distributed load on the top surface. The elements are weightless.

Bounds on values for the dimensionless parameters have been determined from consideration of the possible combinations of arches and soil properties. Where considered appropriate, values have been extended beyond present practice to allow for larger future spans.

Poisson's ratio for steel (ν_m) was assumed to be 0.3. Poisson's ratio for soil (ν_s) appears to vary for structural fills from approximately 0.25 to 0.4, but since this is essentially a second-order variable compared with the other parameters, it was taken to be constant at 0.3. The sensitivity of the response parameters to variation in ν_s is discussed subsequently.

Fill height was considered in terms of the H_f/R_t ratio. Results were obtained over the range 0.1-1.0 for this ratio. As a guide to the desirable ranges for S/H, E_sR_t/EA, and $E_sR_t^3/EI$, data for readily available standard geometries were obtained from catalog LMSS-1976 of ARMCO Inc., Middletown, Ohio. Specifically available spans (S) and heights (H) are plotted in Figure 3 and corresponding ranges for $E_sR_t^3/EI$ and E_sR_t/EA associated with E_s values from 10 to 100 MPa (1450-14 500 psi) are hatched in Figure 4. The specific

points covered by the subsequently developed graphs are indicated by the black dots in Figure 4.

SOURCES OF ERROR

Soil-Metal Slip and Thrust-Beam Effects

Two factors that have potentially significant effects on the response of the structure are the conditions of slip at the soil-metal interface and the presence of thrust beams. A specific study was made to evaluate the relative effects of these factors. The program capabilities permitted a comparison of results for these four cases: (a) no slip and no thrust beams, (b) full slip and no thrust beams, (c) no slip and thrust beams, and (d) full slip and thrust beams. As might be expected, the presence of thrust beams decreased the deflection and increased the thrust (in both cases by about 5 percent). The no-slip condition produced less deflection (by about 6 percent) than the full-slip case. However, greater thrust was associated with no slip only at greater cover heights. At lower cover heights the no-slip condition resulted in less thrust (maximum difference about 5 percent). Most large-span arches constructed to date have incorporated thrust beams, and consequently they were incorporated in the model. The true slip condition lies between full and no slip; the full-slip case was chosen for the model as the more conservative one.

Effect of Variations in Soil Poisson's Ratio

The effect of variations in Poisson's ratio of the soil (ν_s) from the value of 0.3 used in the analysis for the design charts has been investigated. Both the deflection and thrust decrease roughly linearly with increasing ν_s, and vice versa. The increase in deflection is between 7 and 10 percent at $\nu_s = 0.25$. The decrease is from 9 to 13 percent at $\nu_s = 0.35$ and 17 to 25 percent at $\nu_s = 0.40$. Thrust is increased by about 6 percent at $\nu_s = 0.2$ and decreased by about 8 percent at $\nu_s = 0.40$.

The value of 0.3 selected for the design charts is on the low side of values likely to be encountered for good-quality structural fills, and so predicted responses will generally be conservative. Further provision of details for exact determination of the effect of variations in ν_s is considered unwarranted due to the unknown nature of its value in most practical situations.

Nonlinearities

Three basic sources of nonlinearity exist in the large-span corrugated-metal arch problem. They are as follows:

1. Incremental construction nonlinearity--the nature of the construction process produces a progressively changing upper boundary and hence a progressively changing system geometry,
2. Material nonlinearity--the strain for a given stress increment changes depending on the prevailing stress conditions, and
3. Geometric nonlinearity--the deformation of the arch under load produces a progressively changing arch shape.

The approach taken whereby the system response is determined for a series of independent incremental uniform load additions permits consideration of the significant aspects of these effects. The crown deformation and springline thrust are determined separately for each discrete layer. In association with each layer, separate values may be assigned for the system upper boundary and the soil modulus. Summation of the layer responses provides a total response that effectively accounts for the nonlinearities. It has been shown (7) that up to working-load levels the influence of geometric nonlinearity is small.

This approach does not allow for variations in soil modulus arising from differential stress conditions throughout the soil mass. In addition there are potential locations of tensile strains, and the assigned modulus would be inappropriate at these locations. Nevertheless, correlations with results from field studies to date (discussed subsequently) appear to indicate that these factors are of little significance for fill loads up to working-load level. In fact, it appears likely that in most instances a discrete-layer approach that accounts for the changing boundary conditions alone will be sufficient for response prediction. Current methods for prediction of soil modulus provide extremely uncertain parameter values, and until these methods are improved, the higher levels of sophistication appear to be unwarranted.

Effect of Footing Width

Footing widths for these structures are generally determined from consideration of the bearing capacity of the foundation soils. Katona and others (7) have investigated the effect of variations in footing width over the range 0.6-1.3 m (2-4 ft) on the structural response and have found it to be negligible. Displacements vary by about 3 percent and thrusts by about 1 percent.

DESIGN GRAPHS

The design graphs are plotted in Figures 5-16 as a series of pairs indicating the dimensionless deflection parameter ($\delta E_s/pR_t$) and the dimensionless thrust parameter (T/pR_t) versus the fill height ratio (H_f/R_t). There are four groups of 12 graphs at respective S/H ratios of 1.2, 1.4, 1.6, and 1.8. Within each group there are six pairs of graphs corresponding to various values of $E_sR_t^3/EI$, and on each graph is one, two, or three curves for values of E_sR_t/EA.

Analysis of a typical large-span corrugated-metal arch structure is presented to illustrate the procedure for use of the graphs (Figure 17). The fill above crown level is divided into five layers. The deformation and thrust response resulting from the placement of each layer of fill above crown level is determined from the graphs as shown in Table 1.

Consider layer 1 (row 1 in Table 1). Placement of this 1.2-m (4-ft) thick layer brings the fill level to 1.2 m above crown level. The total overburden stress applied to the system by this layer is 23.5 kN/m² (490 psf). Approximate the effect of placement of this layer to that of a uniformly distributed load, equivalent to this overburden stress, applied to the system when the fill level is at the mid-height of the layer. That is, 23.5 kN/m² applied with the fill height (H_f) 0.6 m (2 ft) above crown level. The response under this loading is then determined from the design graphs.

For this configuration, $H_f/R_t = 0.10$, $E_sR_t/EA = 7.9 \times 10^{-2}$, $E_sR_t^3/EI = 9.9 \times 10^3$, and S/H = 1.40. From Figures 9e and 9f, $\delta E_s/pR_t = 2.52$ and $T/pR_t = 1.051$; substituting the known values of E_s, p and R_t, δ = 15.9 mm (0.6 in), and T = 152.1 kN/m (867 lbf·in) [or 17.4 MPa (2522 psi) in terms of plate stress].

The procedure is repeated for successive layers and the response due to each layer is added to that

Figure 5. Deflection and thrust parameters for S/H = 1.2(a-d).

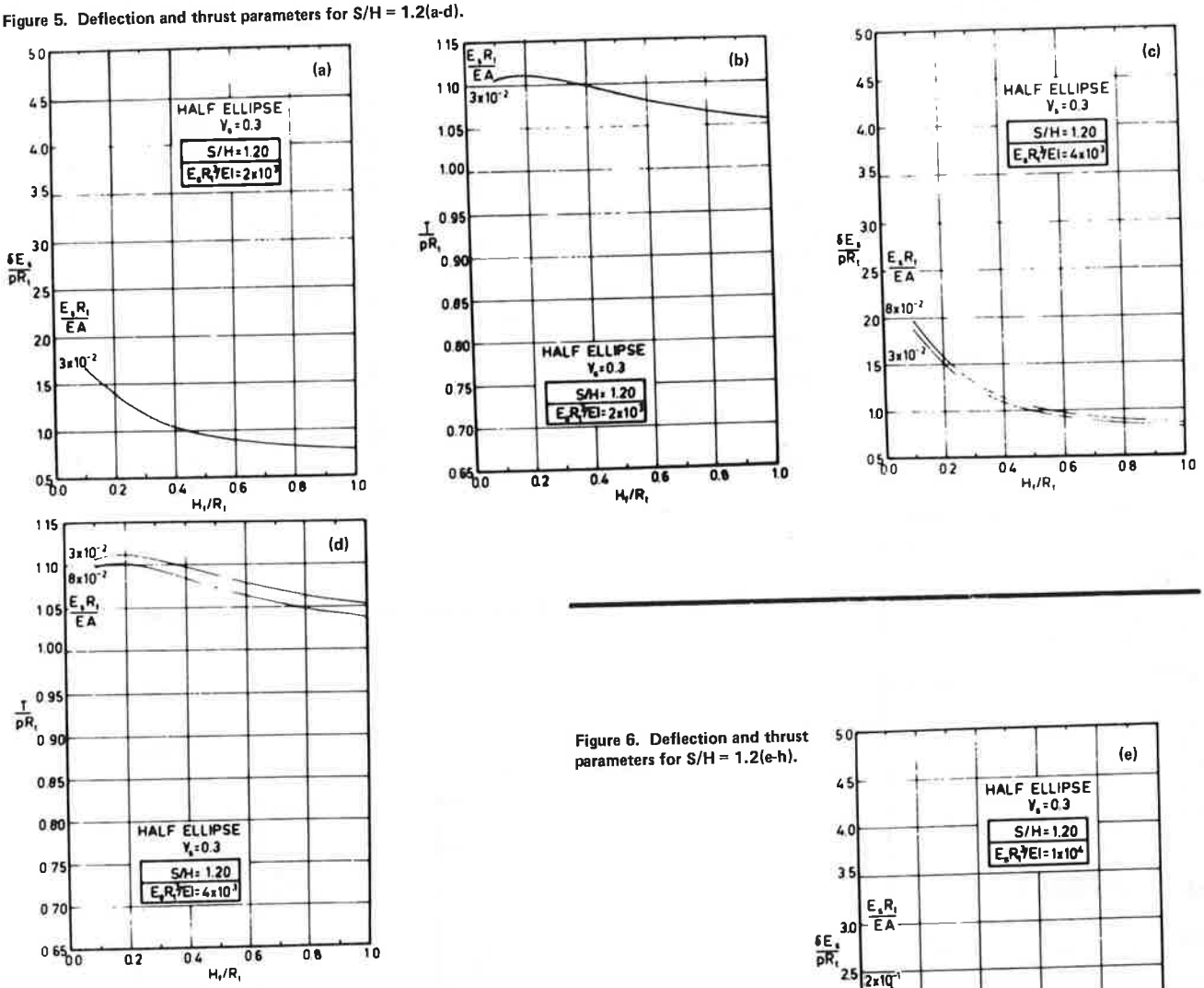

Figure 6. Deflection and thrust parameters for S/H = 1.2(e-h).

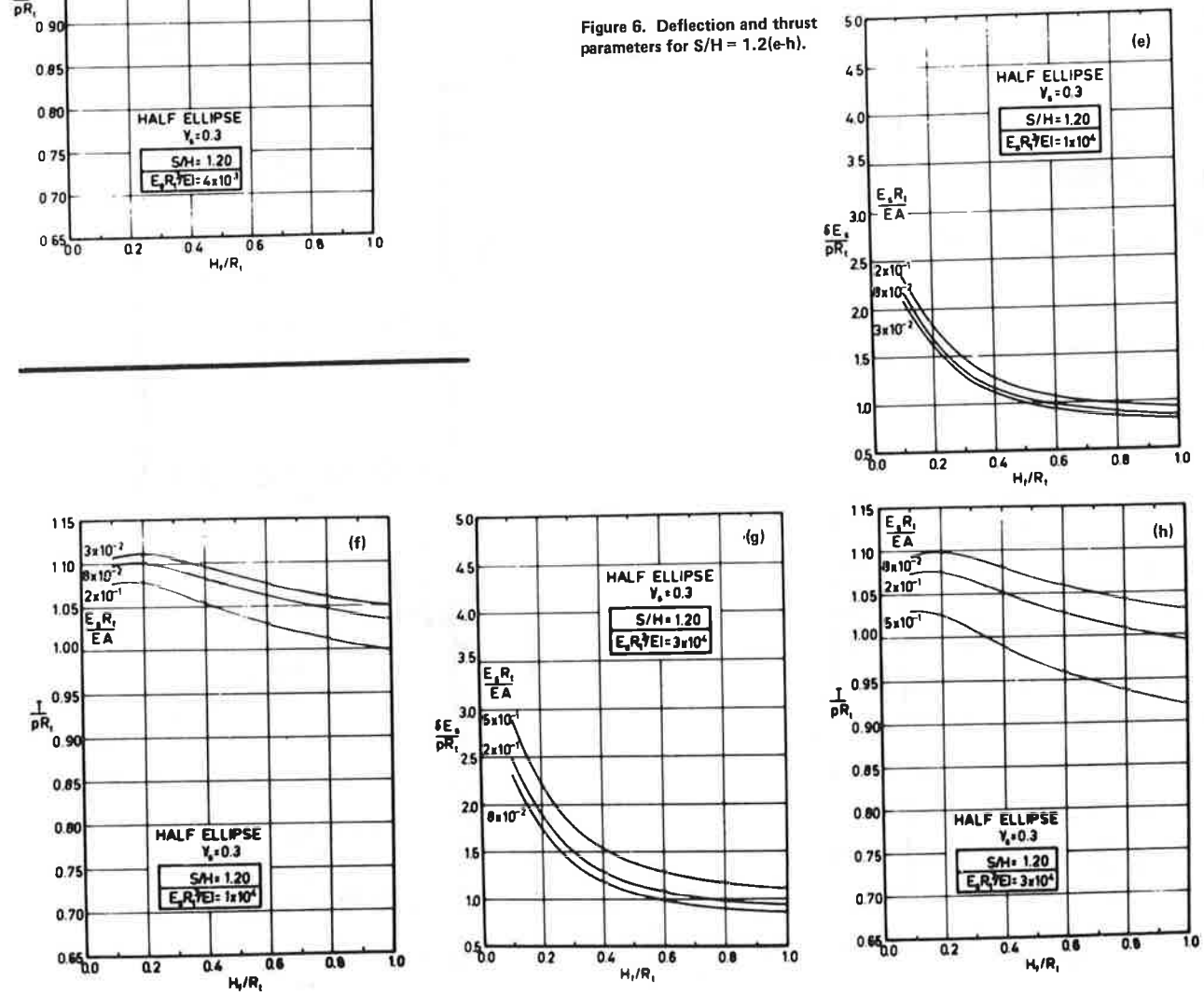

Figure 7. Deflection and thrust parameters for S/H = 1.2 (i-l).

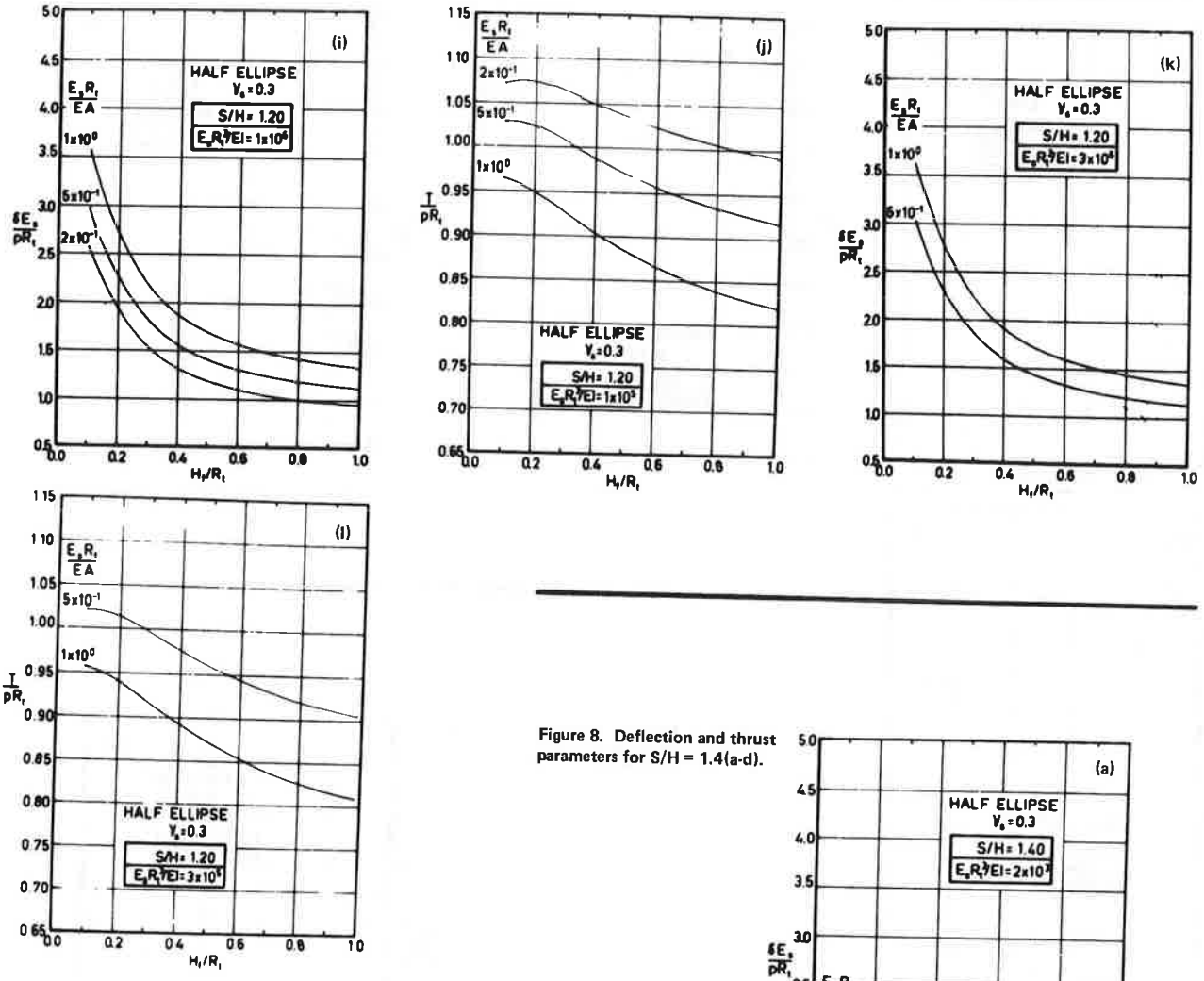

Figure 8. Deflection and thrust parameters for S/H = 1.4(a-d).

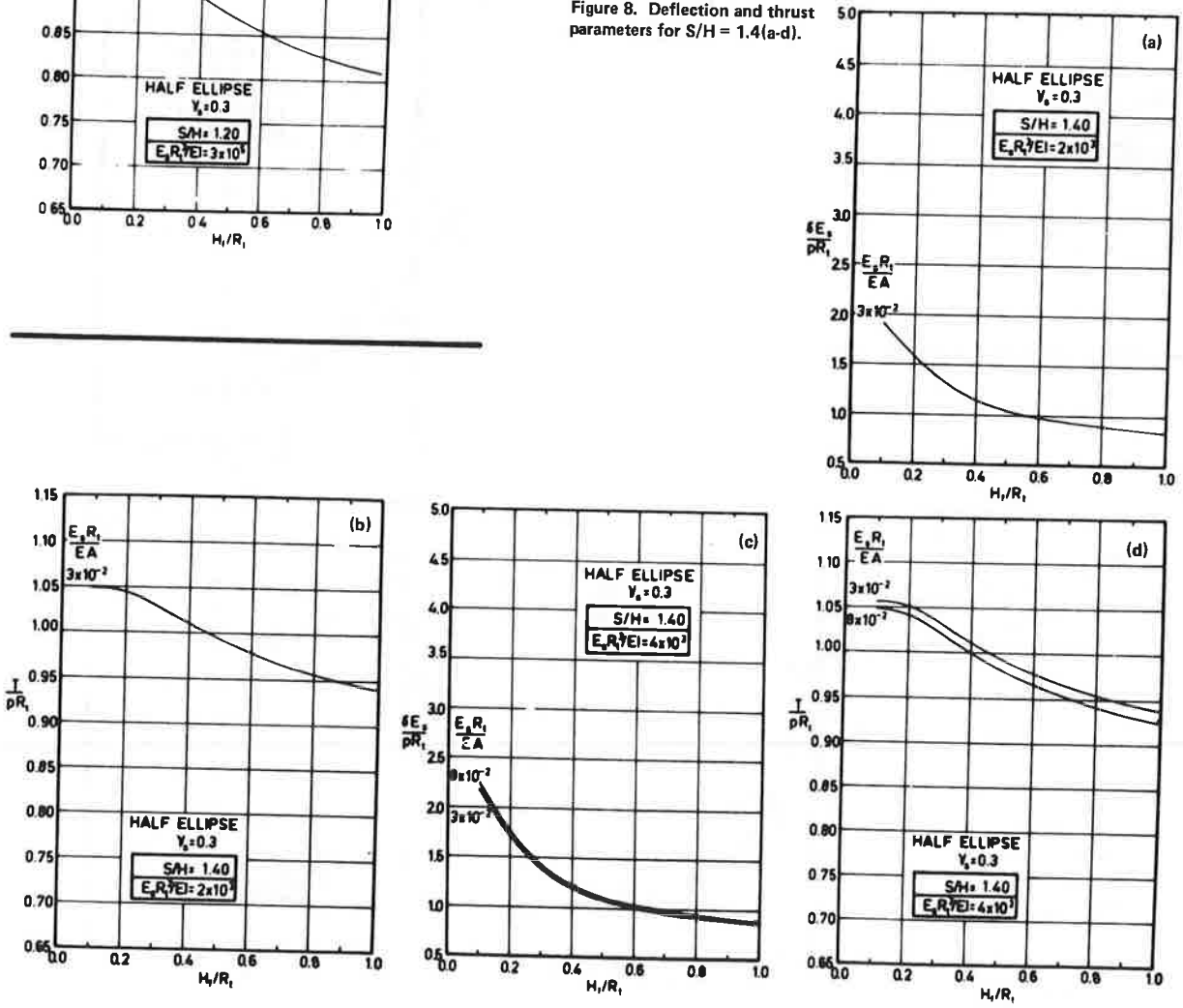

Figure 9. Deflection and thrust parameters for S/H = 1.4(e-h).

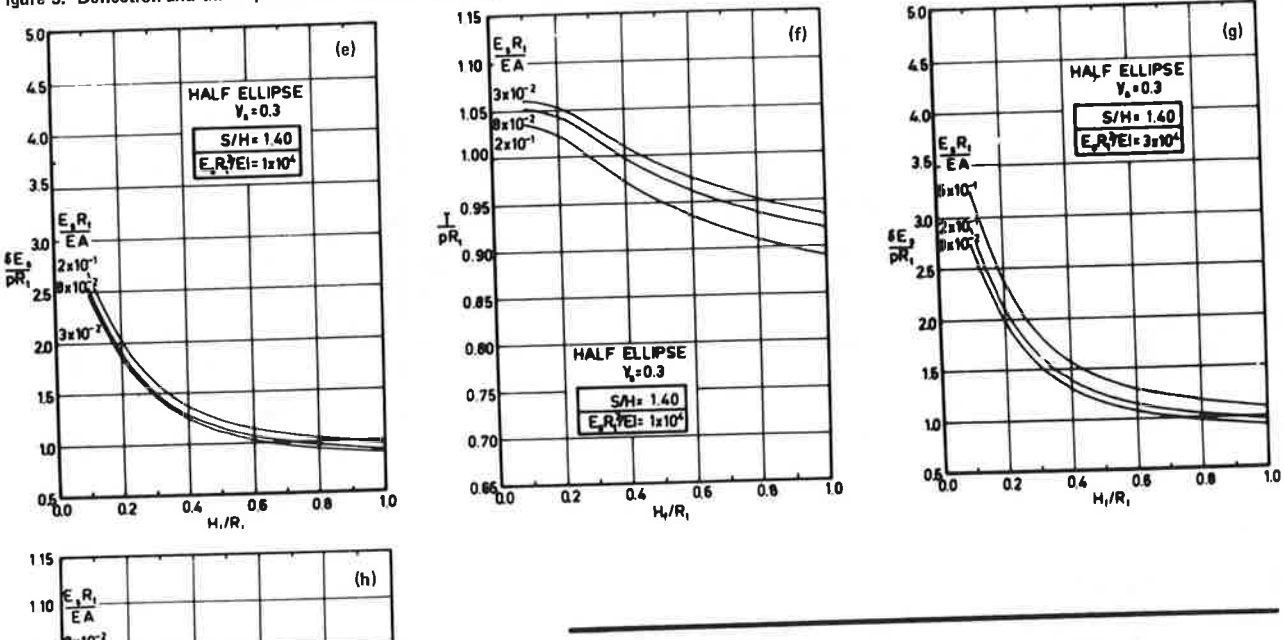

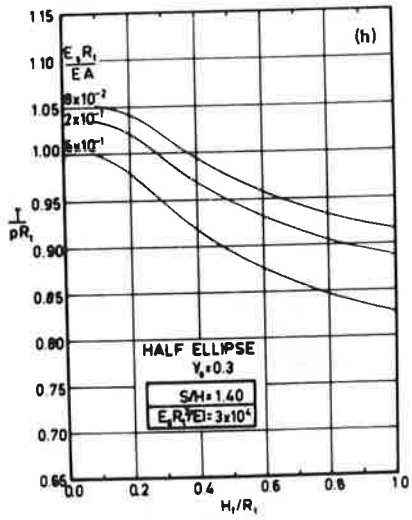

Figure 10. Deflection and thrust parameters for S/H = 1.4(i-l).

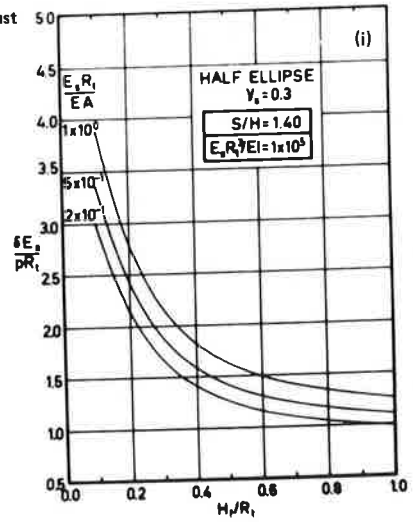

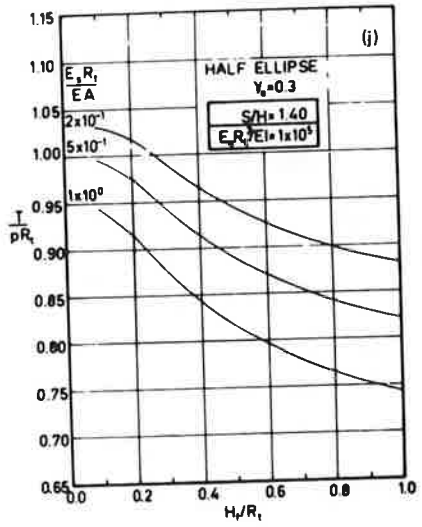

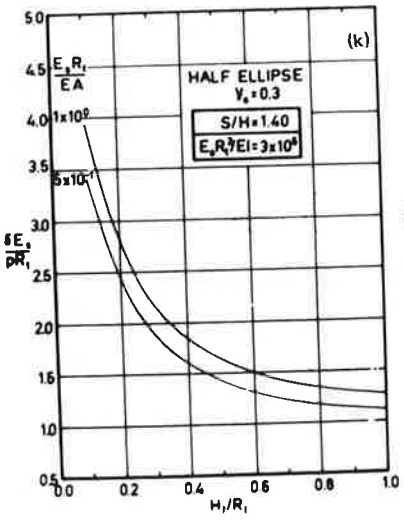

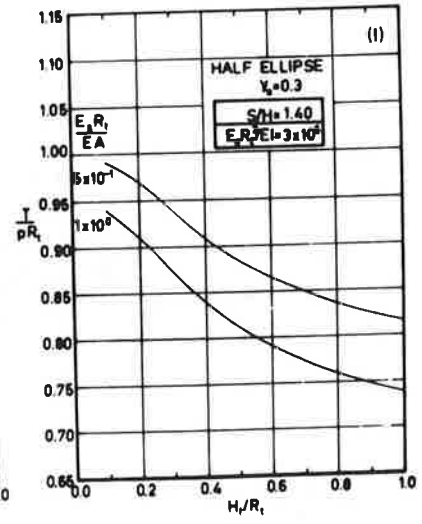

Figure 11. Deflection and thrust parameters for S/H = 1.6(a-d).

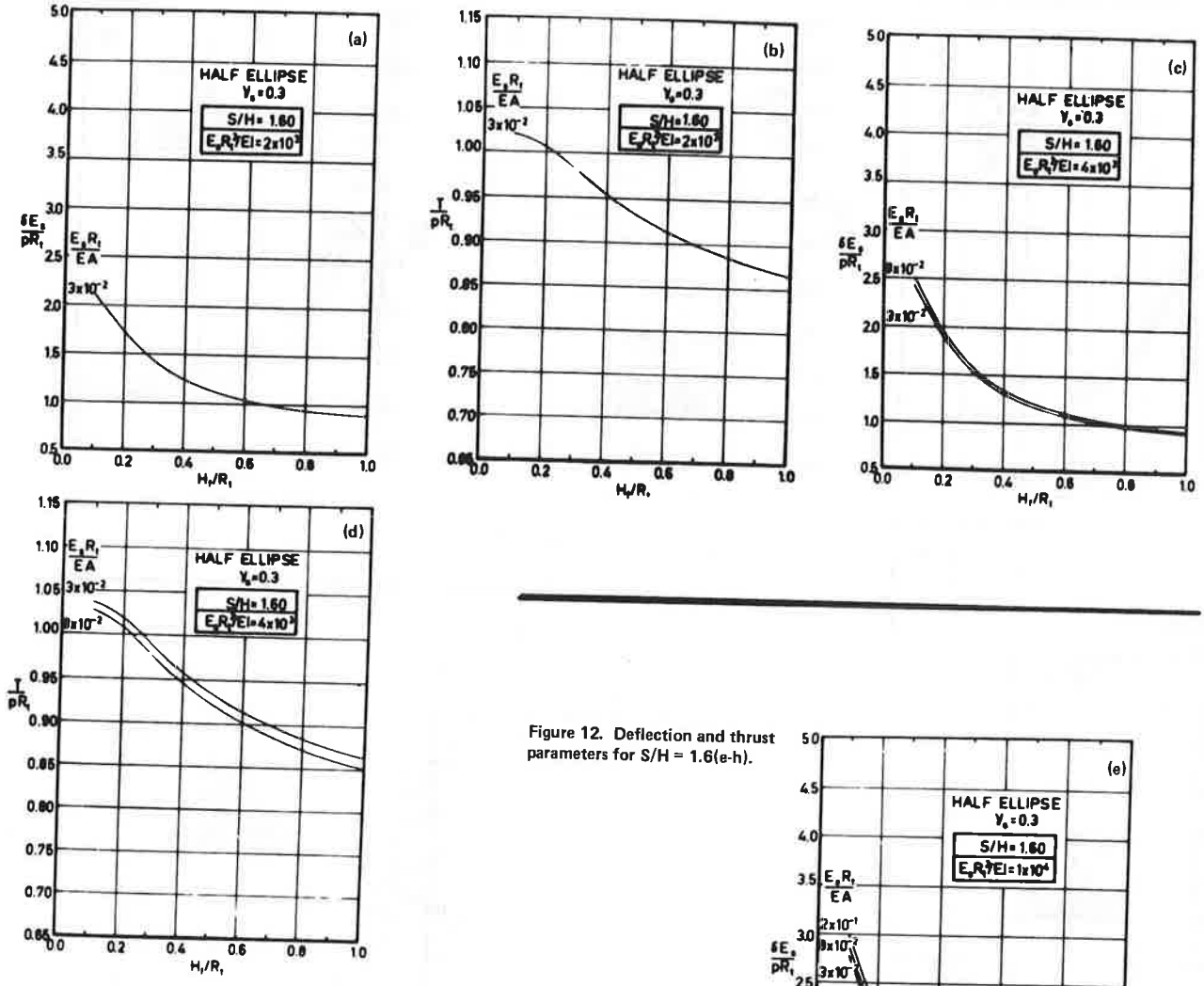

Figure 12. Deflection and thrust parameters for S/H = 1.6(e-h).

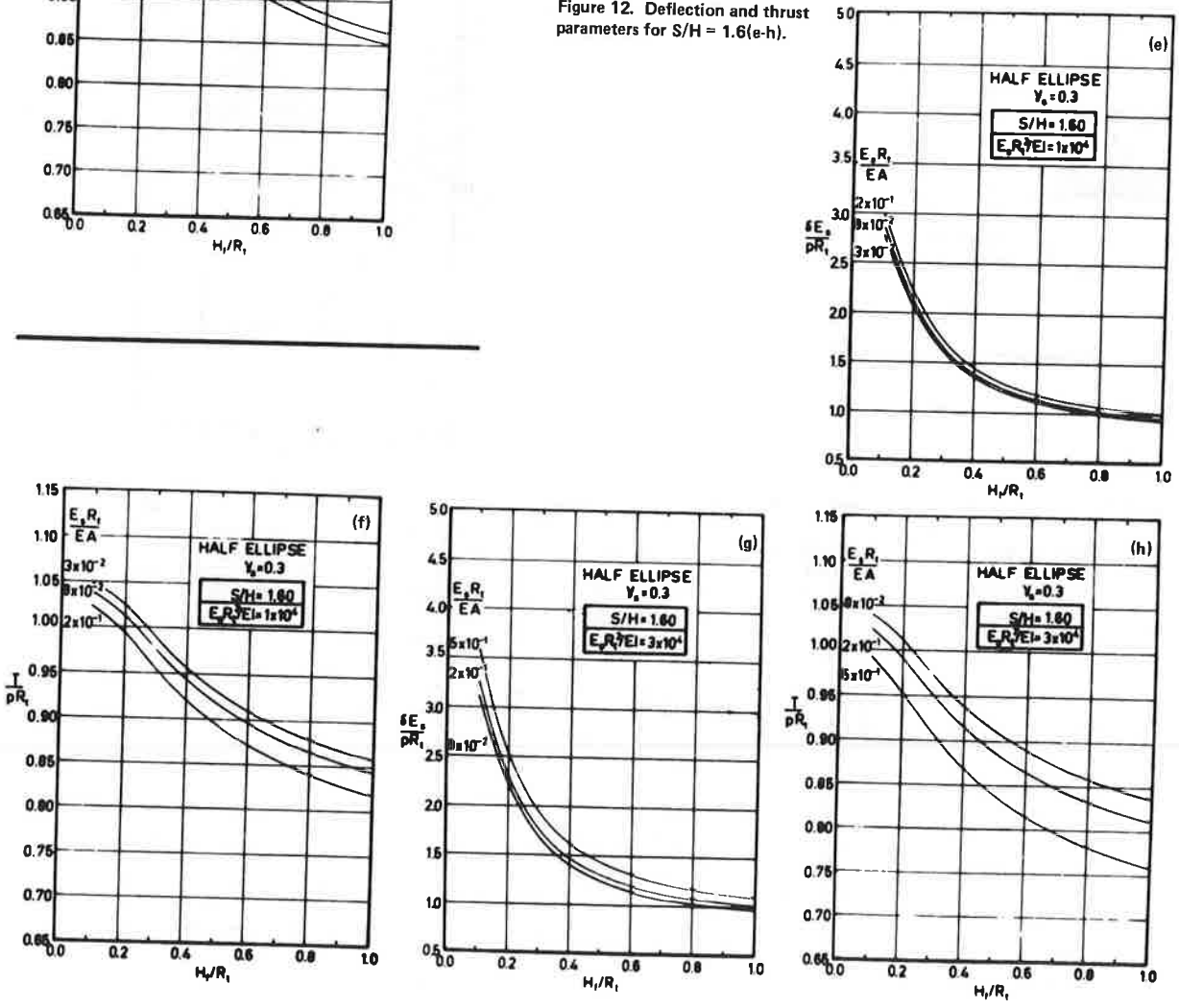

Figure 13. Deflection and thrust parameters for S/H = 1.6(i-l).

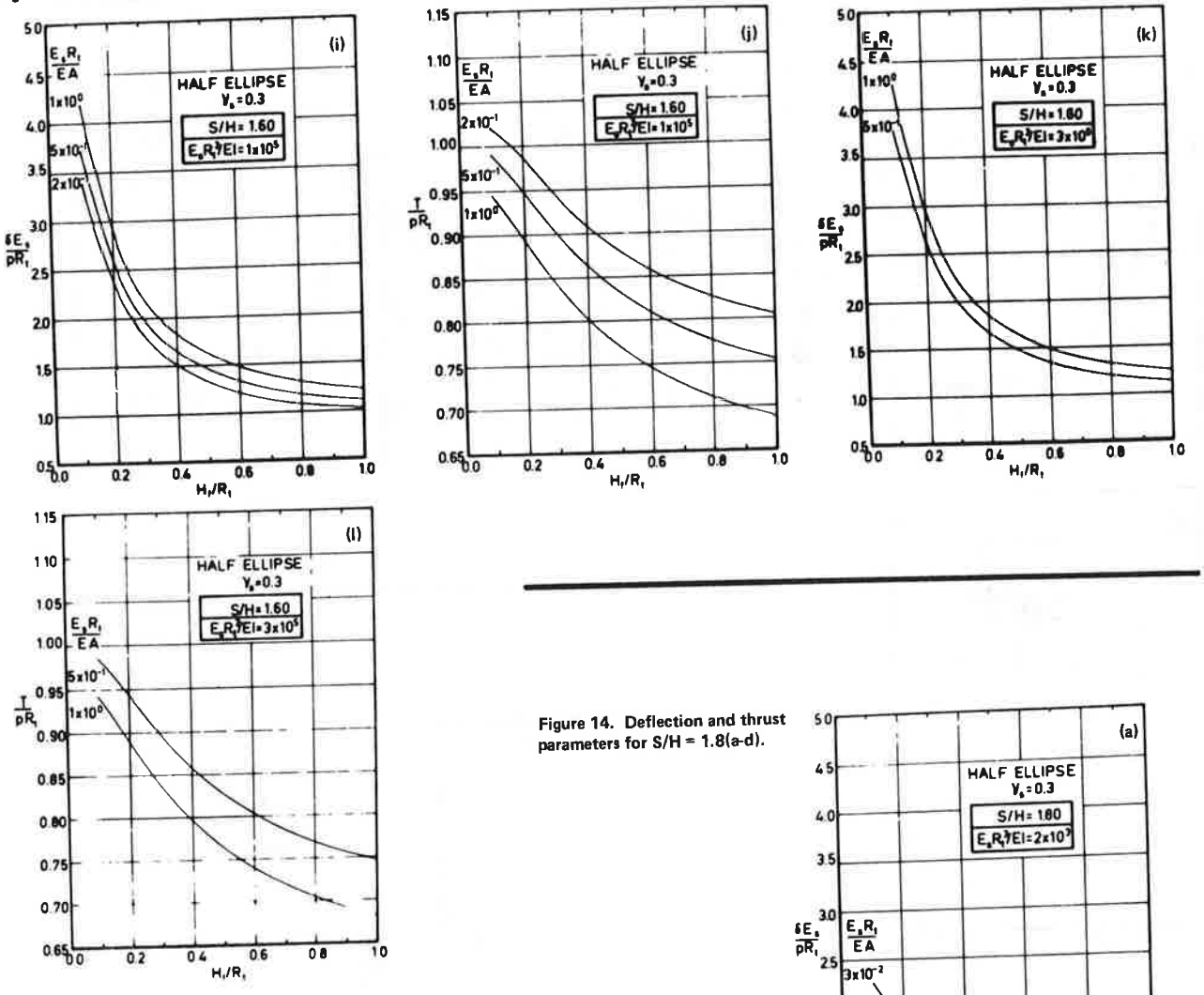

Figure 14. Deflection and thrust parameters for S/H = 1.8(a-d).

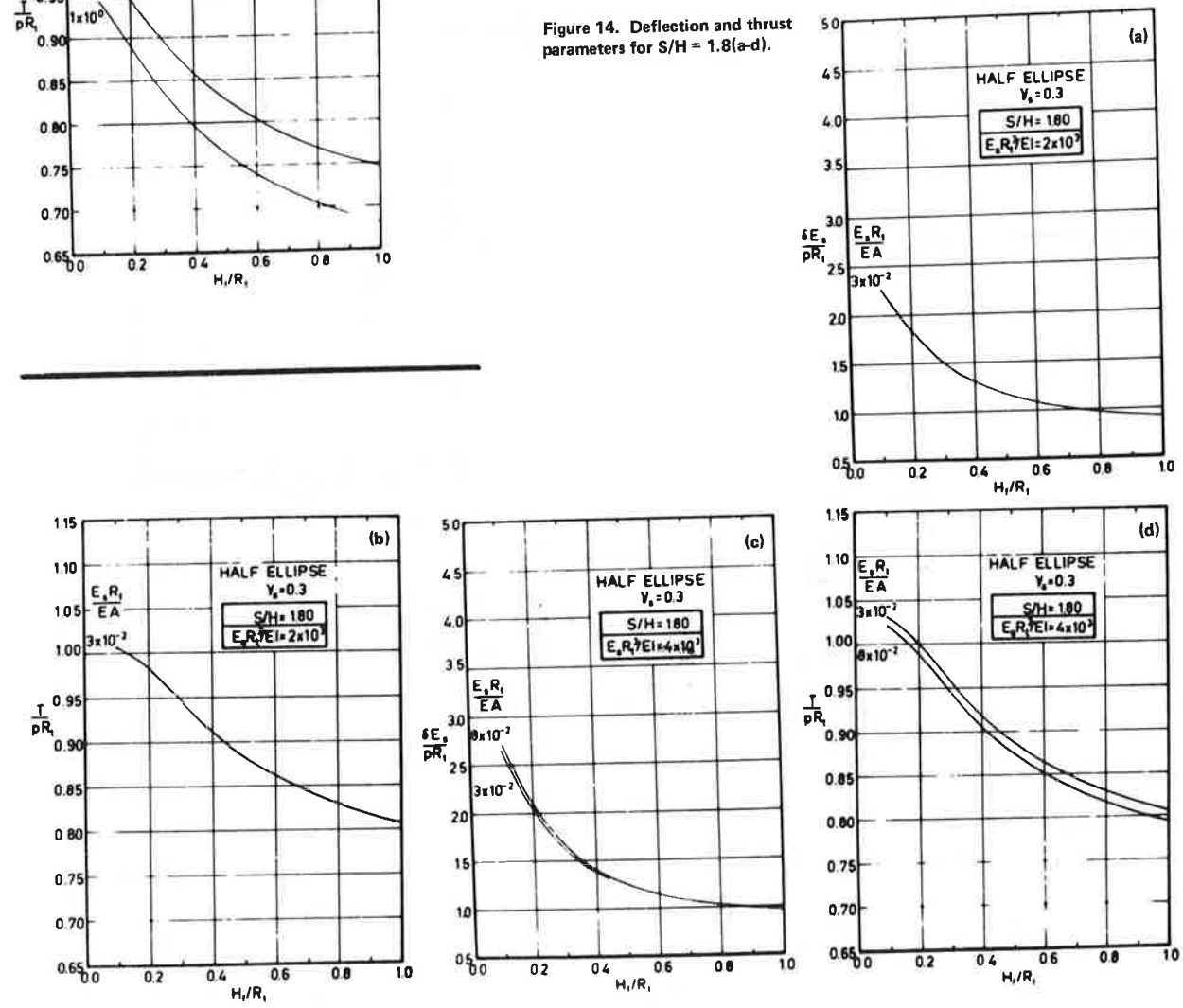

Figure 15. Deflection and thrust parameters for S/H = 1.8(e-h).

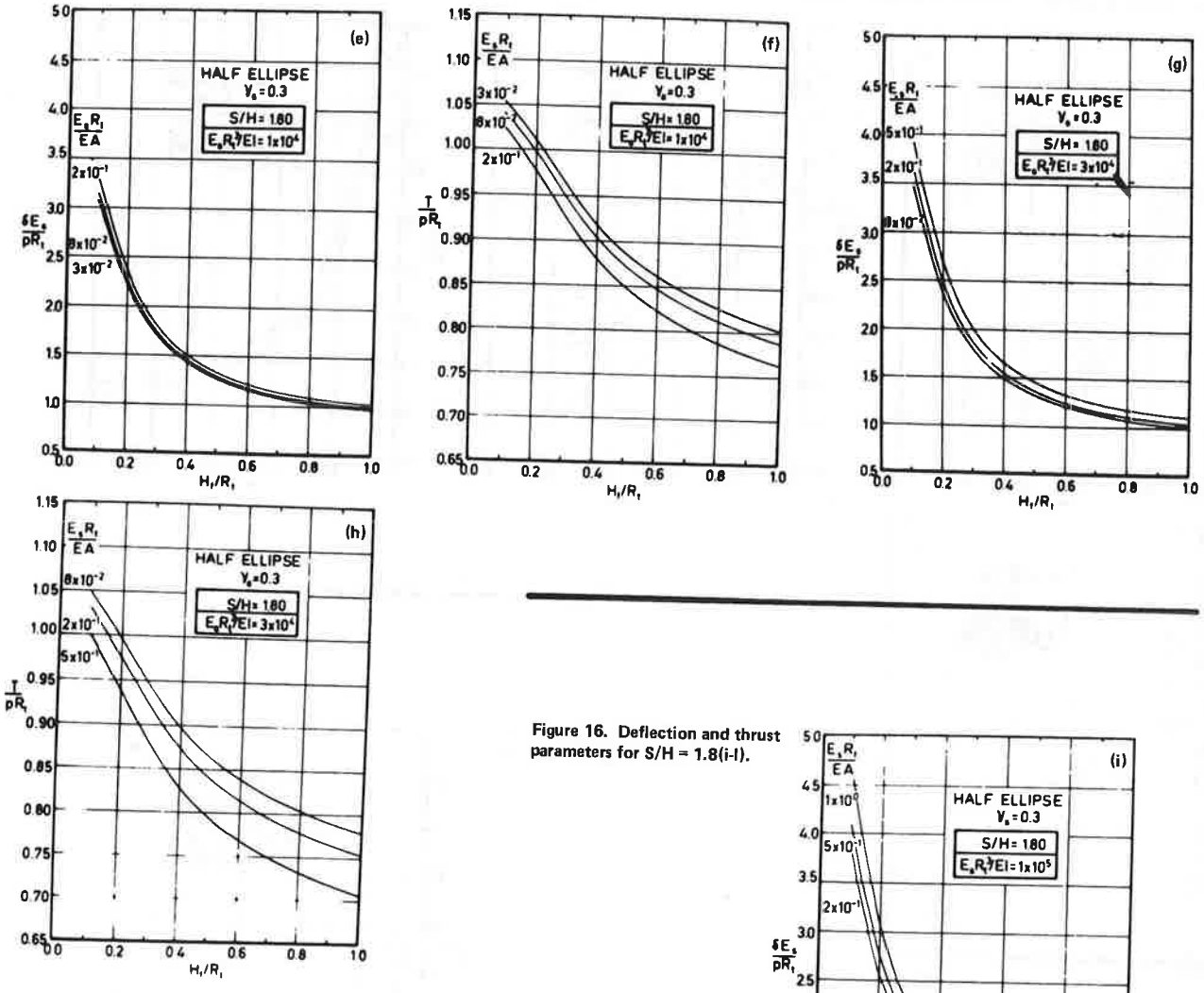

Figure 16. Deflection and thrust parameters for S/H = 1.8(i-l).

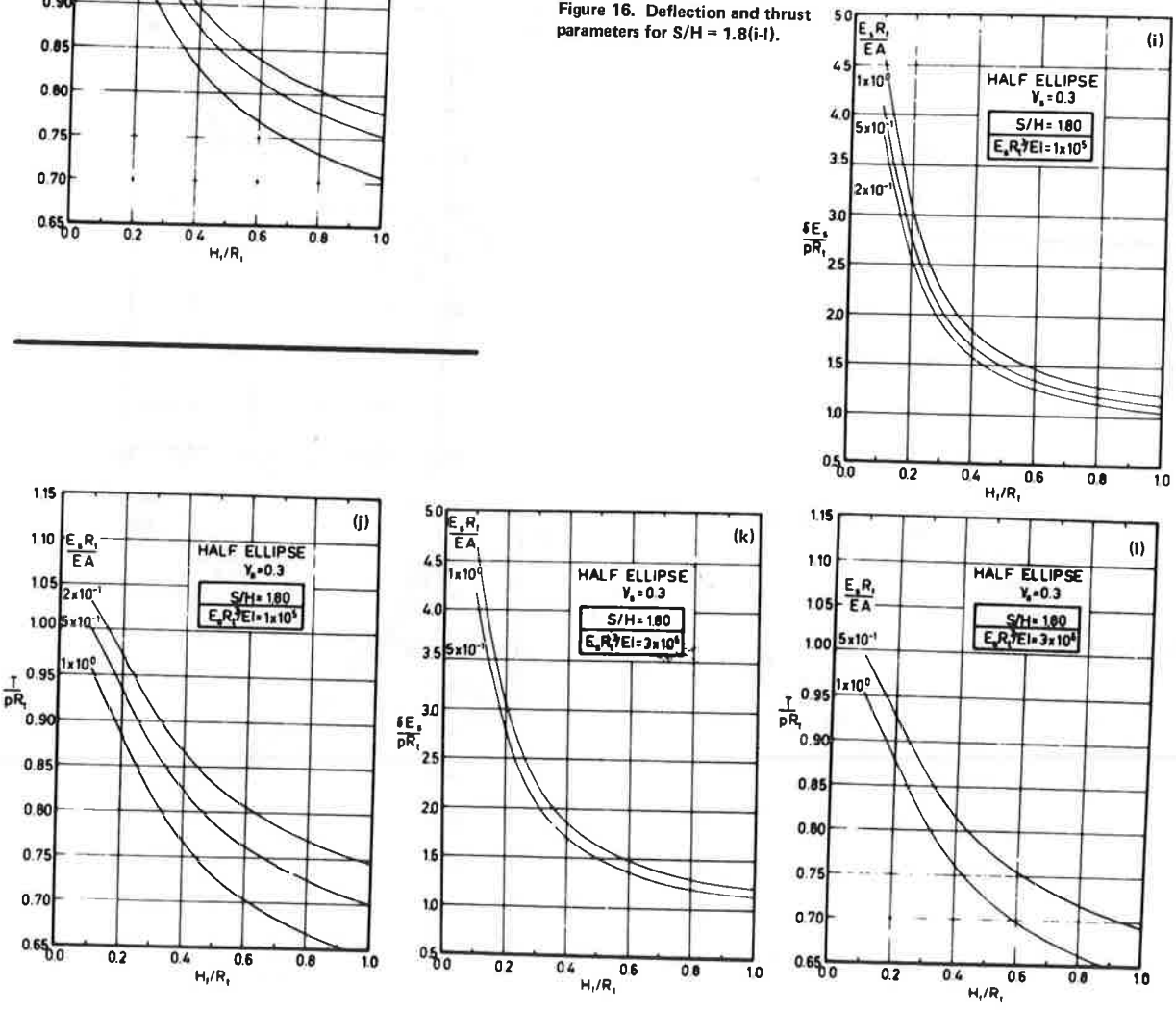

for previous layers to yield the total response for the fill height at the top of each layer. For this typical structure, the predicted total downward crown deflection due to placement of fill above crown level is 45 mm (1.8 in), and the predicted increase in thrust in the steel arch wall at the springline is 715 kN/m (4080 lbf•in).

Figures 18 and 19 show the progressive deflection and thrust, respectively, versus height of fill. It is seen that the deflection response is noticeably nonlinear with respect to fill height, whereas the thrust response is essentially linear. This indicates that deflection is sensitive to the effects of incremental construction, whereas thrust is relatively independent.

Over the linear section of the curves, fewer layers could be used in the analysis to achieve the same result. For example, if the last three layers are combined, the response predictions are altered by less than 1 percent. However, incremental construction nonlinearities are significant in the overall picture. If only a single layer is used, the deflection prediction is almost 20 percent lower than that for five layers.

COMPARISON OF PREDICTIONS WITH FIELD MEASUREMENTS

The validity of this form of analysis as applied to large-span corrugated-metal arch structures is investigated by comparison of predicted and measured performance for a full-scale structure.

Extensive field measurements of the response parameters were taken for a large-span corrugated-metal arch structure built at Leigh Creek, South Australia. Details have been reported by Kay and others (8). The structure consisted of a 12-m (39-ft) span semielliptical arch constructed from 7-mm (5/16-in) corrugated plate, rising 4.7 m (15.4 ft) above tied-back reinforced concrete retaining walls 2.3 m (7.5 ft) high as shown in Figure 20.

The vertical deflection of the crown relative to the footings of the retaining walls and the vertical thrust in the steel arch at the springline on either side were monitored during construction at two sections located at the one-third points along the 26.7-m (87.6-ft) length of the structure. Deflections were measured directly by conventional level surveying, and thrusts were measured indirectly through strain measurements from electrical resistance strain gauges. Continued measurements were only obtained from three of the four relevant strain-gauge stations due to damage at one station during the early stages of construction.

The time for placement of fill above crown level was six days up to a fill height of 1.9 m (6.2 ft). Then there was a break of six weeks before the final 0.2 m (0.7 ft) of fill was placed. During the intervening period, dump trucks of loaded weight about 70 tonnes (77 tons) began crossing the structure.

The soil surrounding the arch consisted of four zones as shown in Figure 20; zone D was the natural foundation soil; zone C, the approach embankments, was constructed from mine spoil with minimal compaction; zones A and B were both constructed with higher-quality material and good compaction. The material used in zone A, closest to the arch, was sand, and in zone B a sandy gravel. The modulus of the zone-A material was determined to be 30 MPa (4350 psi) on the basis of tests on the soil recompacted in the laboratory to the field density. The modulus of the material in zone B was estimated at 30 MPa; that in zone C, 10 MPa (1450 psi); and that in zone D, 40 MPa (5800 psi).

The measured deflection and thrust response are plotted in Figures 21 and 22, respectively, together with response obtained through use of the graphs. Additional data are plotted based on results from a specific finite-element analysis that accounted for the details of the Leigh Creek site such as the tied-back retaining wall, the curved shape of the upper fill boundary, and zones of differing compressibility away from the arch area.

DISCUSSION OF RESULTS

The plotted results in Figures 21 and 22 show much better agreement for prediction of springline thrust

Figure 17. Profile for sample problem.

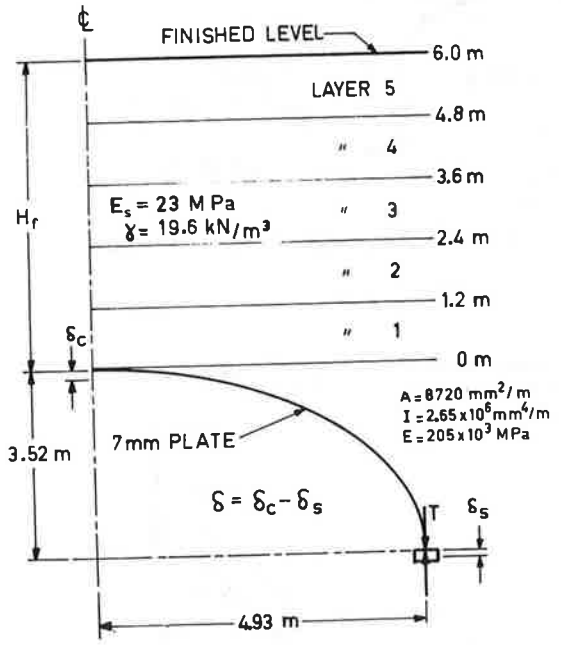

Note: 1 m = 3.3 ft, 1 mm = 0.04 in, 1 MPa = 145 psi, and 1 kN/m³ = 224.8 lbf/ft³.

Table 1. Illustration of procedure.

Layer	Thickness (m)	Fill Level at Top of Layer (m)	Overburden Stress p (kN/m²)	Fill Level at Mid-Height of Layer H_f (m)	H_f/R_t	Data from Graphs		Layer Response	
						$\delta E_s/pR_t$	T/pR_t	δ (mm)	T(kN/m)
1	1.2	1.2	23.5	0.6	0.10	2.52	1.05	15.9	152
2	1.2	2.4	23.5	1.8	0.29	1.50	1.02	9.4	148
3	1.2	3.6	23.5	3.0	0.49	1.15	0.98	7.2	141
4	1.2	4.8	23.5	4.2	0.68	1.01	0.95	6.3	138
5	1.2	6.0	23.5	5.4	0.88	0.93	0.93	5.8	134
Total								44.6	713

Notes: $E_s R_t/EA = 7.9 \times 10^{-2}$; $E_s R_t^3/EI = 9.9 \times 10^3$; S/H = 1.4.
1 m = 3.3 ft; 1 kN/m² = 20 psf; 1 mm = 0.04 in; 1 MPa = 145 psi.

Figure 18. Crown deflection versus fill height for sample problem.

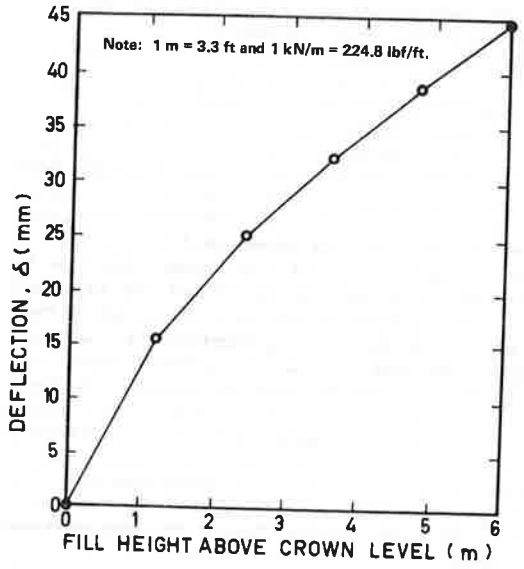

Figure 19. Springline thrust versus fill height for sample problem.

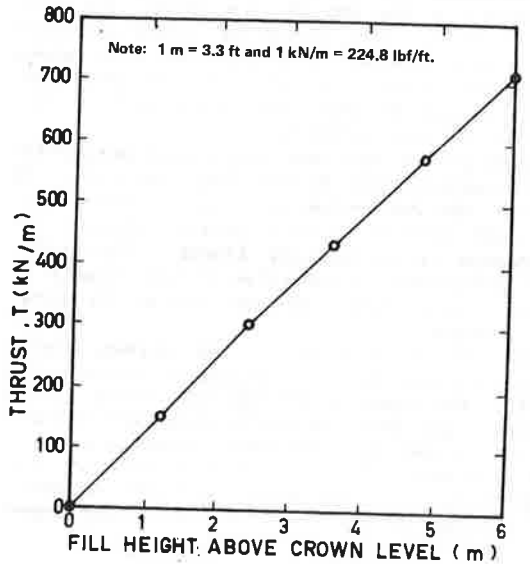

Figure 20. Cross section of instrumented structure at Leigh Creek, South Australia.

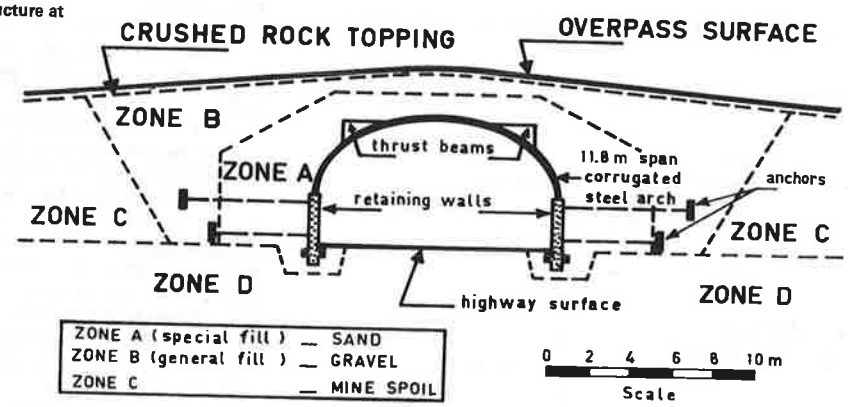

Figure 21. Comparison of results from graphs, specific finite-element program, and field measurements: deflection.

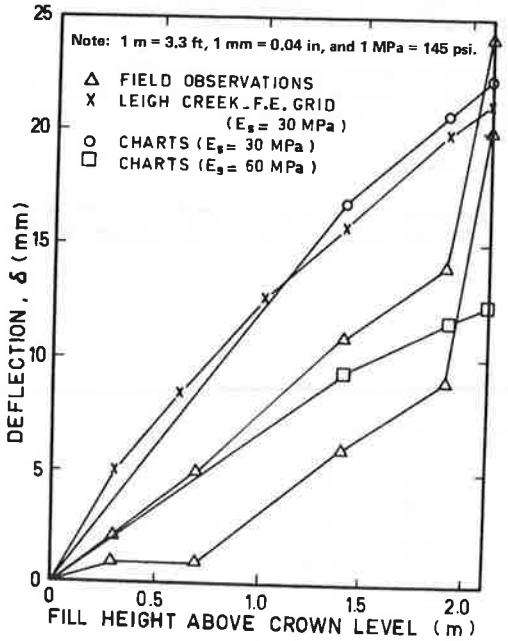

Figure 22. Comparison of results from graphs, specific finite-element program, and field measurements: springline wall stress.

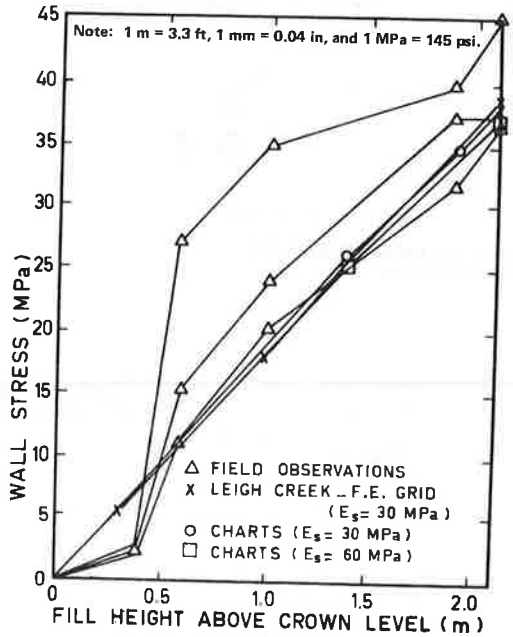

than for prediction of crown deflection. The comparison between results obtained through use of the graphs and those from the specific finite-element analysis was encouraging. For similar values of E_s = 30 MPa the difference in deflection results was 5 percent, whereas the difference in thrust was negligible. This would suggest that the graphs based on the idealized system geometry can be applied to cases where details are somewhat different from the ideal system. Agreement is also demonstrated between predictions of springline thrust and field measurements. Two of the three pertinent strain-gauge results show agreement with predictions within a few percentage points. (It is notable that, for this case, a computation based on the ring compression theory gives a springline thrust that is about 25 percent too low.)

Crown deflection is not predicted with the same level of reliability. Total deflection associated with fill load up to 1.9 m of fill was predicted approximately 70 percent higher than the average measured deflection. (Deflection due to the final 0.2 m of fill could not be separated from that due to heavy-truck loading, according to a paper in this Record by Kay and Flint.) Calculations were based on soil modulus of 30 MPa determined from laboratory triaxial test measurements on the reconstituted granular soil. As demonstrated in Figure 22, a value of E_s = 60 MPa would have given a better estimate. However, it is notable that during the initial fill period over the crown, the measured deflection was small and, in the later stages, the slopes of the as-measured graphs are similar to those of the graphs based on predictions. This performance suggests an explanation in terms of construction procedure. The initial layers of fill placed over the crown do not receive the full compactive effort but are compacted by hand-held equipment. The effect of reduced compaction is considerably greater compressibility of the fill in this zone than the general compressibility, and as the general soil system moves downward with compression of the sidefills, the crown area of the arch, instead of moving downward in a similar fashion, penetrates the zone of more compressible soils. It is likely that improvement to prediction of crown deflection would result if zero deflection were assumed to occur to the level where mechanical compaction has begun. However, further observation of field installations is necessary to justify such an approach.

The effect of the heavy-vehicle live loading on crown deflection is considerable. This is the subject of the paper in this Record by Kay and Flint.

SUMMARY AND CONCLUSION

Graphs have been presented that enable prediction of crown deflection and springline thrust for systems of soil and corrugated-metal arches subject to loads from compacted fills placed above the crown level. Stepwise application of the graphs can minimize errors associated with nonlinear effects for conditions within the working-load range. Comparisons made between predictions based on the graphs and results of field measurements show reasonable agreement.

No recommendations are made concerning criteria for safe design in terms of these aspects of response. Insufficient research on the collapse of such structures has been completed to date to enable suggestions along these lines. Both large-scale testing and analytical work are in progress at the University of Adelaide through which it is hoped to contribute to some preliminary guidelines to a more complete design procedure in the future.

REFERENCES

1. E.T. Selig, J.F. Abel, F.H. Fulhawy, and W.E. Falby. Review of the Design and Construction of Long-Span, Corrugated-Metal, Buried Conduits. FHWA, Interim Rept. FHWA-RD-77-131, 1977.
2. J.G. Abel, G.A. Nasir, and R. Mark. Stresses and Deflections in Soil Structure Systems Formed by Long-Span Flexible Pipe. Department of Civil Engineering, Princeton Univ., Princeton, NJ, Res. Rept. 77-SM-13, 1977.
3. J.M. Duncan. Finite-Element Analysis of Buried Flexible Metal Culvert Structures. Laurits Bjerrum Memorial Volume, March 1975.
4. C.S. Chang, J.M. Espinoza, and E.T. Selig. Computer Analysis of Newtown Creek Culvert. Journal of the Geotechnical Engineering Division of ASCE, Vol. 106, No. GT5, 1980, p. 531.
5. M.G. Spangler. Culverts and Conduits. In Foundation Engineering (G.A. Leonards, ed.), McGraw-Hill, New York, 1962.
6. J.N. Kay and R.C.L. Flint. Design Charts for Large-Span Metal Arch Culverts. Department of Civil Engineering, Adelaide Univ., Australian Road Res. Board, Interim Rept., 1978.
7. M.G. Katona, D.F. Meinhart, T. Orillac, and C.H. Lee. Structural Evaluation of New Concepts for Long-Span Culverts and Culvert Installations. FHWA, Interim Rept. FHWA-RD-79-115, 1979.
8. J.N. Kay, D.L. Avalle, R.C.L. Flint, and C.F.R. Fitzhardinge. Instrumentation of a Corrugated Steel-Soil Arch Overpass at Leigh Creek, South Australia. Proc., 10th Conference of Australian Road Res. Board, Vol. 10, No. 3, 1980, pp. 57-70.

Publication of this paper sponsored by Committee on Subsurface Soil-Structure Interaction.

Analysis of Live-Load Effects in Soil-Steel Structures

GEORGE ABDEL-SAYED AND BAIDAR BAKHT

This paper is based on an analytical study undertaken to complement a previously reported experimental study on live-load effects in the metallic shell of a soil-steel structure. An account of load dispersion above the conduit cannot be made by neglecting the presence of the conduit. The plane-strain approach of analyzing a soil-steel structure is found to be a defensible one even for concentrated loads. It is found that the manner of load dispersion in the longitudinal direction of the conduit is distinctly different from that in the transverse direction. This observation confirms previously reported experimental results. A simplified method, which at best is a crude approximation, can only pick up the maximum thrust values in the conduit wall and is dependent on the con-